

October 13, 1988

HEAVY FLAVOR PRODUCTION AT FIXED TARGET AND COLLIDER ENERGIES* CONF-8808145-23

The submitted manuscript has been authored by a contractor of the U.S. Government under contract No. W-31-109-ENG-38. Accordingly, the U.S. Government retains a nonexclusive, royalty-free license to publish or reproduce the published form of this contribution, or allow others to do so, for U.S. Government purposes.

ANL-HEP-CP--88-67

DE89 005862

EDMOND L. BERGER
High Energy Physics Division
Argonne National Laboratory
Argonne, IL 60439

ABSTRACT

A review is presented of heavy quark production in $\bar{p}p$, π^-p , and pp interactions at fixed target and collider energies. Calculations of total cross sections are described including contributions through next-to-leading order in QCD perturbation theory. Comparisons with available data on charm and bottom quark production show good agreement for reasonable values of charm and bottom quark masses and other parameters. Open issues in the interpretation of results are summarized. A discussion is presented of signatures, backgrounds, and expected event rates for top quark production.

1. Introduction

The specification of reliable cross sections for heavy quarks, including their production spectra in longitudinal and transverse momentum, and comparisons with data test the quantum chromodynamic (QCD) mechanisms by which all heavy objects are expected to be produced. Strategies in the search for new flavors such as top are predicated on best estimates of cross sections and of momentum distributions in phase space not only of the new flavor but, perhaps more importantly, of lighter flavors which contribute deceptive backgrounds. Those considering hadronic experiments to establish flavor-antiflavor mixing and possible CP violation require a detailed understanding of expected production spectra.

A significant result reported during the past year was the completion [1] of a calculation of the heavy flavor production cross section through order α_s^3 in QCD perturbation theory. Here α_s^3 is the running coupling strength in QCD. Explicit comparisons with data have also been made [2,3]. In this paper I will summarize comparisons of the $O(\alpha_s^3)$ cross sections with data on hadroproduction of charm and bottom. The $O(\alpha_s^3)$ contributions are larger in many cases of interest than the $O(\alpha_s^2)$ terms. Not yet available are $O(\alpha_s^3)$ distributions in transverse momentum

*Work supported by the U.S. Department of Energy, Division of High Energy Physics, Contract W-31-109-ENG-38.

To be published in the Proceedings of the 1988 Annual Meeting of the Division of Particles and Fields, Storrs, Connecticut, August 15-18, 1988

DISTRIBUTION OF THIS DOCUMENT IS UNLIMITED

MASTER

for values of transverse momentum $p_{T,Q}$ greater than the quark mass m_Q . These are eagerly awaited inasmuch as the $O(\alpha_s^3)$ $Q\bar{Q}$ jet contributions provide different event topologies [4,5] and may be very much larger than the $O(\alpha_s^2)$ contributions when $p_{T,Q} \gg m_Q$. These distributions are important, especially at collider energies, for a proper estimation of the bottom quark background to a possible top quark signal.

In Section 2, I provide a brief summary of the results of the $O(\alpha_s^3)$ computation. Comparisons with data on charm production and on bottom production are presented in Secs. 3 and 4. Comments on top quark production are made in Sec. 5, and conclusions are summarized in Sec. 6.

2. Total Cross Sections

In hadron hadron interactions, the lowest order parton-parton subprocesses leading to production of a pair of heavy quarks are $q\bar{q} \rightarrow Q\bar{Q}$ and $gg \rightarrow Q\bar{Q}$. The square of the invariant matrix element for these two-to-two subprocesses is proportional to α_s^2 , where $\alpha_s = g^2/4\pi$ and g is the coupling strength in QCD. In QCD, α_s is a logarithmic function of the renormalization/evolution scale Q , which is only determined to be of order the mass m_Q of the heavy quark. Additional subprocesses enter in the next order in the QCD perturbation expansion. These include $q\bar{q} \rightarrow Q\bar{Q}g$, $gg \rightarrow Q\bar{Q}g$, $gq \rightarrow Q\bar{Q}g$, and $g\bar{q} \rightarrow Q\bar{Q}g$.

The total cross section for $ab \rightarrow Q\bar{Q}X$, the inclusive production of a pair of heavy quarks, is

$$\sigma_{ab}(s) = \sum_{ij} \int dx_1 \int dx_2 f_i^a(x_1, Q^2) f_j^b(x_2, Q^2) \hat{\sigma}_{ij}(\hat{s}, Q^2). \quad (1)$$

In this equation, $f_i^a(x_1, Q^2)$ represents the density of partons of type i in incident hadron a ; $\hat{s} = x_1 x_2 s$ is the square of the energy in the parton-parton collision. The hard scattering cross section $\hat{\sigma}_{ij}$ is written as

$$\hat{\sigma}_{ij}(\hat{s}, Q^2) = \frac{\alpha_s^2(Q^2)}{m_Q^2} F_{ij} \left(\rho, \frac{Q^2}{m_Q^2} \right), \quad (2)$$

where $\rho = 4m_Q^2/\hat{s}$. The dimensionless functions F_{ij} are expressed in the form

$$F_{ij} \left(\rho, \frac{Q^2}{m_Q^2} \right) = F_{ij}^{(0)}(\rho) + 4\pi\alpha_s(Q^2) \left[F_{ij}^{(1)}(\rho) + \bar{F}_{ij}^{(1)}(\rho) \ln \frac{Q^2}{m_Q^2} \right] + O(\alpha_s^2). \quad (3)$$

Explicit expressions for the set of functions $F_{ij}^{(0)}$, $F_{ij}^{(1)}$, and $\bar{F}_{ij}^{(1)}$ may be found in Ref. 1.

Several sources of uncertainty beset attempts to make definite predictions. These include choice of the heavy quark mass; choice of parton densities (particularly the gluon density); and specification of the evolution scale Q^2 . The last is an intrinsic theoretical uncertainty. Since there is only one scale in the problem, it is "natural" to expect Q to lie in the range $m_Q/2 \lesssim Q \lesssim 2m_Q$. In this report I

will show results for different choices of Q^2 , $Q^2 = m_Q^2$ and $Q^2 = 4m_Q^2$. When the cross section is computed to order α_s^3 , changes in Q in the vicinity of m_Q result in "errors" of order α_s^4 . These differences are not always small. There appears to be no general evidence for the choice of an optimized evolution scale for heavy flavor production [3].

3. Hadroproduction of Charm

In Fig. 1 I present calculations of cross sections for charm quark production in pp interactions at fixed target energies [2]. The first point to be made is that the QCD contributions in order $O(\alpha_s^3)$ are large. The ratio K of the full cross section computed through order α_s^3 to the result obtained in lowest order, order α_s^2 , is defined as

$$K = \sigma(O(\alpha_s^2) + O(\alpha_s^3)) / \sigma(O(\alpha_s^2)). \quad (1)$$

Values of K are typically 3 for charm production in π^-p and pp interactions at fixed target energies. It has been known for some years that the lowest order calculations in QCD provide cross sections which are significantly below experimental measurements. The large increase provided by the $O(\alpha_s^3)$ contributions helps to remedy this discrepancy.

The data in Fig. 1 are from the LEBC-EHS [6] and LEBC-MPS [7] experiments. Beginning with the measured D/\bar{D} inclusive and $D\bar{D}$ pair cross sections, Goshaw [8] obtained estimates of the cross sections for $pp \rightarrow c\bar{c}X$. His values are $\sigma(pp \rightarrow c\bar{c}X) = 14$ to $23 \mu\text{b}$ at $p_{\text{lab}} = 400 \text{ GeV}/c$ and 29 to $55 \mu\text{b}$ at $p_{\text{lab}} = 800 \text{ GeV}/c$. Cross sections have been determined in many other experiments. However, I choose not to show them in Fig. 1 because many of those measurements were made with nuclear targets, and the precise nuclear A dependence is not known in each case.

A glance at Fig. 1 shows the considerable sensitivity of predictions to the choices of the charm quark mass m_c and of the parton densities. For a given set of parton densities, a decrease of the mass from $m_c = 1.5 \text{ GeV}$ to $m_c = 1.2 \text{ GeV}$ results in an increase in cross section by about a factor of three. For a given m_c , there is about a factor of two increase in predicted cross section when the Duke-Owens [9] set 1 (DO 1) parton densities are used instead of the Martin-Roberts-Stirling [10] set 1 (MRS 1). Since the $c\bar{c}$ cross section is proportional to α_s^2 , a substantial fraction of the difference of predicted yields is attributed to the different values of Λ in the DO 1 and MRS 1 parametrizations [2].

At the ISR energies of $\sqrt{s} = 63 \text{ GeV}$, we may use the DO 1 ($m_c = 1.5 \text{ GeV}$) and MRS 1 ($m_c = 1.2 \text{ GeV}$) curves in Fig. 1 to bracket uncertainties from below and above. I estimate that $\sigma(pp \rightarrow c\bar{c}X; \sqrt{s} = 63 \text{ GeV})$ lies most likely in the range of 55 to $100 \mu\text{b}$. Even with $O(\alpha_s^3)$ contributions included, it is difficult to accommodate a charm cross section greater than $\sim 130 \mu\text{b}$ at $\sqrt{s} = 63 \text{ GeV}$.

Calculations for $\pi^-p \rightarrow c\bar{c}X$ are presented in [2]. The results in Fig. 1 and those for $\pi^-p \rightarrow c\bar{c}X$ [2] demonstrate that defensible QCD calculations reproduce the magnitude of the measured total charm cross section at fixed target energies.

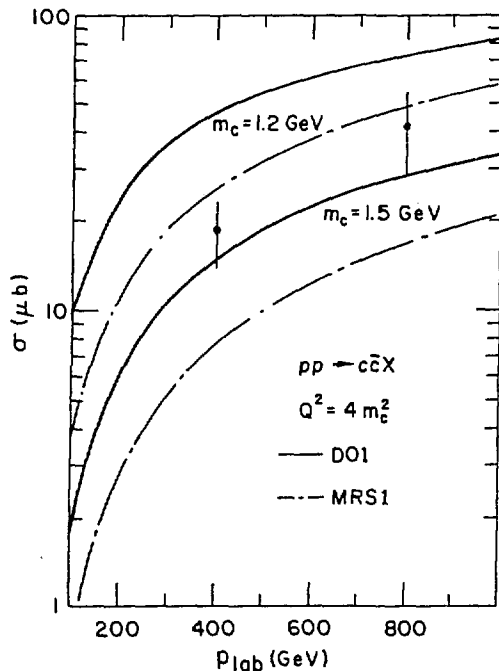


Fig. 1. Cross sections for $pp \rightarrow c\bar{c}X$ as a function of the laboratory momentum for two choices of the charm quark mass m_c and two different sets of parton densities. I obtained these results from the full QCD expression [1] through order α_s^3 ; the evolution scale Q^2 was chosen as $Q^2 = 4m_c^2$. The data at $p_{\text{lab}} = 400$ and 800 GeV are from the LEBC-EHS [6] and LEBC-MPS [7] experiments.

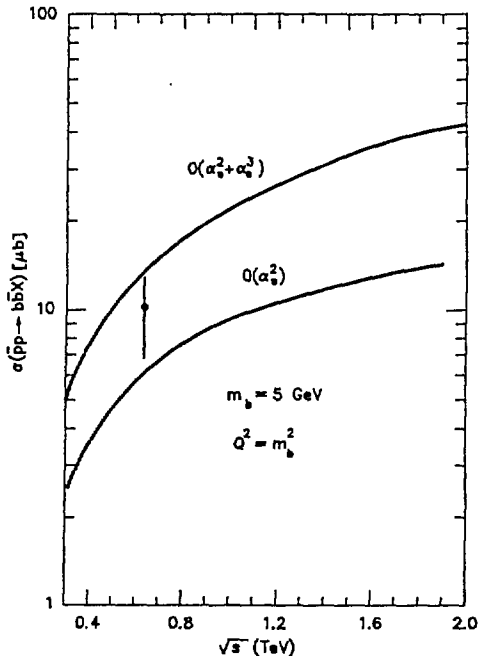


Fig. 2. Calculations of bottom quark production in proton-antiproton collisions as a function of \sqrt{s} . I show both the full answer through order α_s^3 and the lowest order $O(\alpha_s^2)$ result for $m_b = 5$ GeV and evolution scale $Q^2 = m_b^2$. The Duke-Owens set 1 parton densities were used. The one datum is from the CERN UA1 collaboration [11].

However, because of the sensitivity to the choice of the parton densities, we cannot use the results to “pin down” the charm quark mass appropriate in perturbative calculations to better than $1.2 < m_c < 1.5$ GeV. It does appear possible, however, to discard a mass as large as $m_c = 1.8$ GeV. The agreement between theory and data in Fig. 1 is an indication that charm production may be on the way towards being “understood” in terms of perturbative QCD. There are several open issues [2], however, including: discomfort with the large size of the K factor; leading particle effects in the experimental longitudinal momentum distribution of charm particles, $d\sigma/dx_F$, not reproduced by perturbative calculations of charm quark production; the nuclear dependence of charm production; and higher-twist effects known to be important in deep-inelastic lepton scattering for values of $Q^2 \simeq 4m_c^2$.

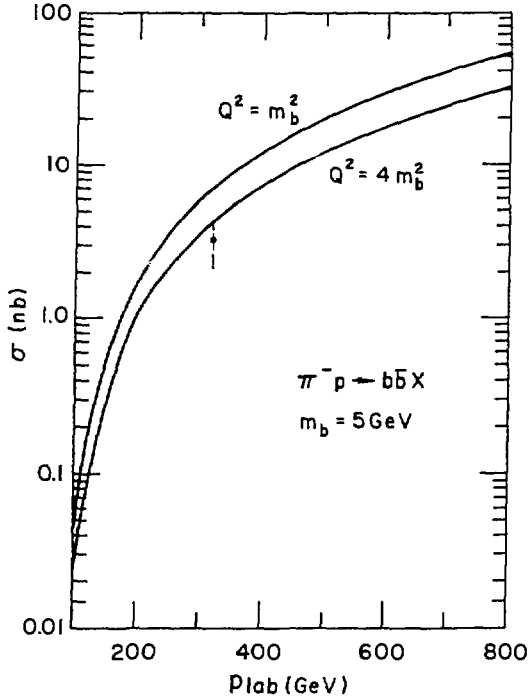


Fig. 3. Cross section through order α_s^3 for bottom quark production in $\pi^- p$ interactions as a function of laboratory momentum. Here $m_b = 5$ GeV, and two choices are made for the evolution scale, $Q^2 = m_b^2$ and $Q^2 = 4m_b^2$. The one datum is the result reported by the WA78 collaboration [12].

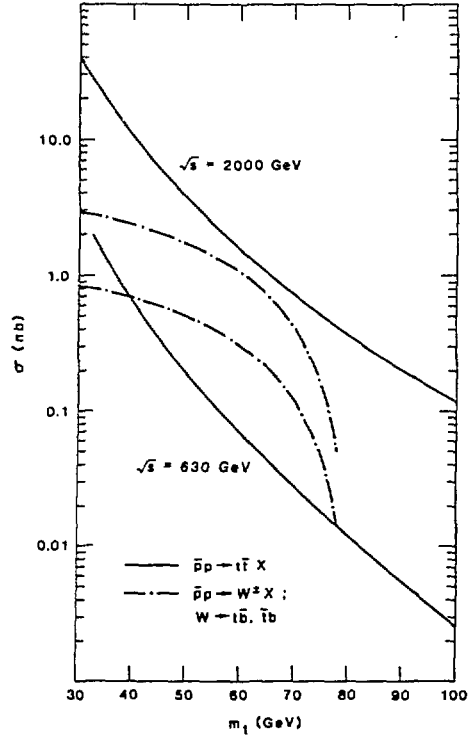


Fig. 4. Expected cross sections as a function of the mass of the top quark at $\sqrt{s} = 630$ GeV and $\sqrt{s} = 2$ TeV [4,5], order α_s^2 only.

4. Hadroproduction of Bottom

In Figs. 2 and 3 calculations of $b\bar{b}$ pair cross sections are shown as a function of energy in $\bar{p}p$ and $\pi^- p$ interactions [2]. Results for $pp \rightarrow b\bar{b}X$ may be found in [2]. As in the case of charm discussed in Sec. 3, the contributions in order α_s^3 are significant. This point is illustrated in Fig. 2 for $\bar{p}p \rightarrow b\bar{b}X$ at collider energies. At fixed target energies the value of K in pp interactions is larger than that in $\pi^- p$ interactions, related to the more important role of gluon initiated subprocesses in pp interactions [2].

At $\sqrt{s} = 630$ GeV, there is not a large spread in predictions associated with the choice of different parton densities—the lowest and highest predictions shown in Table 5 of Ref. [2] are $9.5 \mu\text{b}$ and $12.8 \mu\text{b}$. This is a small effect when compared with the large ($\sim \times 3$) increase in predicted cross section in going from $O(\alpha_s^2)$ to

$O(\alpha_s^3)$, as shown in Fig. 2. For bottom production at $\sqrt{s} \gtrsim 300$ GeV, the pp and $p\bar{p}$ cross sections are nearly equal. The only measurement of bottom production at $p\bar{p}$ collider energies is that reported by the UA1 collaboration based on an analysis of dimuon production. The $b\bar{b}$ pair cross section extrapolated to all phase space [11] is $\sigma(p\bar{p} \rightarrow b\bar{b}X) = 10.2 \pm 3.3 \mu\text{b}$ in fine agreement with expectations.

In Fig. 3, I present results for the total $b\bar{b}$ pair cross section in π^-p interactions at fixed target energies for a particular choice of bottom quark mass $m_b = 5$ GeV. The one datum on Fig. 3 is the measurement of the CERN WA78 collaboration [12]. Originally the WA78 group had published [13] a value of $\sigma(\pi^-N \rightarrow b\bar{b}X; p_{\text{lab}} = 320 \text{ GeV}) = 4.5 \pm 1.4 \pm 1.4$ nb per nucleon. Subsequent reevaluations were made of their overall normalization reference as well as of their acceptance and efficiency based on a model which incorporates production properties in transverse and longitudinal momenta consistent with those predicted [4,14] in perturbative QCD. These improvements result in a reduction of the cross section [12] to $3.27 \pm 0.24 \pm 0.9$ nb per nucleon. Another group [15] has reported observation of a signal consistent with bottom production and quotes a "model dependent $b\bar{b}$ production cross section" $\sigma(\pi^-N \rightarrow b\bar{b}X; p_{\text{lab}} = 286 \text{ GeV}) = 14_{-6}^{+7}$ nb per nucleon, considerably larger than that of the CERN WA78 collaboration. The model adopted by the NA10 group to simulate $B\bar{B}$ production is questionable [2].

The calculations shown in Fig. 3 are appropriate for $\pi^-p \rightarrow b\bar{b}X$ whereas the one datum is derived from interactions on a uranium target. The theoretical results should be modified for the fact that the target is a mixture of neutrons and protons. This effect was studied in Ref. 5 where I showed that the cross section per average nucleon is *smaller* than the cross section for production from proton targets; the factors are 0.68, 0.80, and 0.87 at $p_{\text{lab}} = 200, 400, \text{ and } 600$ GeV/c.

Of greatest interest for cross sections computed through order α_s^3 is sensitivity to the choice of evolution scale Q^2 . For $\pi^-p \rightarrow b\bar{b}X$ in the momentum range 300 to 600 GeV/c, there is about a factor of two decrease in the total cross section when the evolution scale is increased from $Q^2 = m_b^2$ to $Q^2 = 4m_b^2$. Comparison with the datum in Fig. 3 favors the choice $Q^2 = 4m_b^2$ if $m_b = 5$ GeV. Over the range $400 < p_{\text{lab}} < 1000$ GeV/c, the expected cross section $\sigma(pp \rightarrow b\bar{b}X)$ is decreased by about a factor of two when the b quark mass is increased from $m_b = 5$ GeV to 5.4 GeV and increased by about a factor of two if the b quark mass is decreased from 5 GeV to 4.6 GeV [4,5].

5. Top Quark

For a fixed value of \sqrt{s} , the contributions through $O(\alpha_s^3)$ in perturbative QCD result in smaller increases in predicted yields as the quark mass is increased. For example, at $\sqrt{s} = 630$ GeV, *typical* K factors [1] are in the range $1.2 \lesssim K \lesssim 1.7$ for a top quark of mass $m_t = 40$ GeV and $1.1 \lesssim K \lesssim 1.3$ for $m_t = 80$ GeV. At $\sqrt{s} = 1.8$ TeV, the numbers [1] are $1.3 \lesssim K \lesssim 1.8$ at $m_t = 40$ GeV and $1.2 \lesssim K \lesssim 1.7$ at $m_t = 80$ GeV.

Based on a detailed analysis of events in which muons are observed at large transverse momentum in coincidence with hadronic jets, the UA1 collaboration

derived a lower limit of 44 GeV at 95% confidence level for the mass of the top quark [16]. This value has been reduced slightly to 41 GeV in Ref. [3]. A better determination of the bound from the data requires that the correct $O(\alpha_s^2)$ distributions in rapidity and transverse momentum be used in the simulation programs both for top production and for the backgrounds from bottom and charm production.

In addition to the hadronic mechanisms discussed in this review, production through decay of intermediate vector bosons must also be considered; e.g. $\bar{p}p \rightarrow W^\pm X$, $W \rightarrow t\bar{b}$ and $\bar{p}p \rightarrow Z^0 X$, $Z^0 \rightarrow t\bar{t}$. Cross sections are presented in Fig. 4 as a function of the mass of the top quark [4,5]. At the CERN collider energy of $\sqrt{s} = 630$ GeV, the intermediate W mechanism is dominant for $40 < m_t < 78$ GeV. At Fermilab Tevatron collider energies, hadronic production is dominant for all values of m_t . For an expected integrated luminosity of 1 pb^{-1} at $\sqrt{s} = 1.8$ TeV, the cross sections in Fig. 4 correspond to the production of 10^4 $t\bar{t}$ pairs if $m_t = 40$ GeV and 100 $t\bar{t}$ pairs if $m_t = 100$ GeV.

A favorite signature for top production is the identification of an isolated lepton (e or μ) plus at least two hadronic jets. The overall branching fraction for the decay $t \rightarrow b\ell\nu$; $\bar{t} \rightarrow$ hadronic jets is $2 \times 2 \times (1/9) \times (2/3) \simeq 0.3$ ($\ell = e$ or μ).

The severity of backgrounds is best appreciated by an examination of the integral transverse momentum spectrum $\sigma_b(p_{T,b} > p_{T,b}^{\min})$ for bottom quark production. Motivated by the notion that a bottom quark moving with large $p_{T,b}$ will yield a decay lepton whose transverse momentum is comparable to that arising from the decay of a slowly moving but more massive quark, we may compare $\sigma_b(p_{T,b} > m_t)$ with $\sigma_t(p_{T,t} > 0)$. As shown in Refs. [4,5], when only the lowest order QCD contributions are retained, $\sigma_b(p_{T,b} > 40 \text{ GeV}) > \sigma_t(p_{T,t} > 0, m_t = 40 \text{ GeV})$. Thus, even in lowest order, the distribution in transverse momentum of leptons at large $p_{T,\ell}$ is likely to be dominated by backgrounds from the semi-leptonic decay of b and c quarks. Further selections are needed to achieve a signal to background ratio approaching unity. Particularly promising appears to be the distribution in an isolation variable, I , where I is a measure of the total energy within a cone of solid angle about the direction of the identified lepton [16]. For light quarks moving with large transverse momentum, it is likely that hadronic energy associated with the secondary quark (e.g. c in $b \rightarrow \ell\nu c$) will be folded forward into the cone of solid angle about the direction of ℓ . Correspondingly, I will be large. By contrast, for decay of a massive t quark, $t \rightarrow \ell\nu b$, there is a greater chance of that the lepton ℓ will be isolated in phase space, resulting in a peak near $I = 0$. Precise predictions of the distributions in I associated with both the signal and backgrounds require a refined understanding of the dynamics of the semi-leptonic decay process $Q \rightarrow \ell\nu q$.

In their case study of the production of a possible top quark with mass $m_t = 40$ GeV, the UA1 collaboration [16], determined that a selection $I < 2$, in conjunction with other important selections, was necessary to achieve a signal to background ratio of 2 or greater. After all selections are imposed, the UA1

efficiency for detecting a top quark in the muon channel is 4.6% for a top quark mass of 40 GeV. By implication, about 50 events will be retained of the 10^4 $t\bar{t}$ events expected in the 1 pb^{-1} sample at $\sqrt{s} = 1.8 \text{ TeV}$. The efficiency is expected to improve as m_t is increased.

In previous cases, new flavors have been identified through the observation of distinctive bound states, the J/ψ and Υ families. In the analysis described above, the distinguishing signal for top quark production is a peak in the isolation variable I for small I . It seems desirable to find a more robust discriminating signal for top.

If $m_t > m_W$, the dominant background appears to arise from the QCD production of W 's in association with hadronic jets [17]. Unconventional decays of the top would make detection even more difficult. These include $t \rightarrow bH^+$, $H \rightarrow \tau\nu$ or $c\bar{s}$ [18] and $t \rightarrow \tilde{t}\tilde{\gamma}$, $\tilde{t} \rightarrow b\tilde{W}$ [19]. Here H^+ denotes a possible charged Higgs particle, and \tilde{t} denotes the supersymmetry partner of the top quark.

6. Conclusions and Discussion

Heavy flavor production has been advanced to a new level of precision in perturbative QCD now that full next-to-leading order calculations have been completed. The contributions in order α_s^3 are large in many cases of practical interest. These calculations offer the potential of better agreement with data on charm quark production, but they also raise questions about convergence of the expansion of the cross section in perturbative QCD.

Applicability of the perturbative results requires that the mass of the heavy flavor be "large". Whether charm, with $1.2 < m_c < 1.5 \text{ GeV}$, satisfies this restriction is not clear. Issues include a quantitative understanding of the nuclear A dependence of charm production and quantitative estimates of the role of (additive) higher twist terms, proportional to $1 \text{ GeV}/m_Q$ and expected to be substantial for charm production. The size of the $O(\alpha_s^3)$ contributions introduces a new condition of applicability of the perturbative results. The contributions are particularly significant when the integration over phase space is dominated by values of the parton-parton subenergy *either* close to threshold, $\hat{s} \sim 4m_Q^2$, *or* very large, $\hat{s} \gg 4m_Q^2$. Correspondingly, predictions will be most stable in restricted intervals of $2m_Q/\sqrt{s}$. According to these criteria, predictions for top quark production at the current collider energies of $\sqrt{s} = 630 \text{ GeV}$ and $\sqrt{s} = 1.8 \text{ TeV}$ would seem particularly reliable, as would those for bottom quark production at Fermilab fixed target energies. It is desirable to develop an understanding and/or techniques which will lead to confidence in calculations extended into the regions $\sqrt{s} \gg 2m_Q$ and/or $\sqrt{s} \simeq 2m_Q$.

If the reservations discussed above are set aside, the calculations through order α_s^3 may be compared with data on charm production at fixed target energies, as was done in Sec. 3. Good agreement is obtained for values of m_c in the range $1.2 < m_c < 1.5 \text{ GeV}$. Uncertainties include the choice of Λ_{QCD} , the magnitude and shape of the gluon density $g(x, Q^2)$ in the relevant interval of x , and the choice of the evolution scale Q^2 in both α_s and the parton densities. Only much

more precise data over a broad range of energies will permit tighter bounds on the "parameter set" (m_c , Q^2 , Λ , and $g(x, Q^2)$). Measurements of correlations in rapidity between a produced Q and \bar{Q} will provide valuable additional checks on production dynamics [14]. They may be particularly valuable in the case of charm production for separating perturbative effects from those associated with final state interactions.

This review was focussed on cross sections integrated over all phase space. The calculation of cross sections differential in transverse momentum and valid for $p_{T,Q} \gg m_Q$ requires perturbative techniques appropriate for a problem with two large momentum scales, here, $p_{T,Q}$ and m_Q . Such results are essential for a full understanding of the charm and bottom quark backgrounds to the signal associated with yet heavier quarks.

Acknowledgments

I have benefitted from discussions with R. K. Ellis and A. B. Wicklund. Research done at Argonne National Laboratory is supported by the Department of Energy, Division of High Energy Physics, Contract W-31-109-ENG-38.

References

1. P. Nason, S. Dawson, and R. K. Ellis, Nucl. Phys. **B303**, 607 (1988); see also W. Beenakker, H. Kuijf, W. L. Van Neerven, and J. Smith, Stony Brook report ITP-SB-88-13.
2. E. L. Berger, "Heavy Flavor Production", Argonne report ANL-HEP-CP-88-26, to be published in the Proceedings of the Advanced Research Workshop on QCD Hard Hadronic Processes, St. Croix, October, 1987.
3. G. Altarelli, M. Diemoz, G. Martinelli and P. Nason, CERN report CERN-TH 4978/88.
4. E. L. Berger, Nucl. Phys. B (Proc. Suppl.) **1B**, 425 (1988).
5. E. L. Berger, in *Hadrons, Quarks, and Gluons*, Proceedings of the XXII Rencontre de Moriond, Les Arcs, France, edited by J. Tran Thanh Van (Editions Frontières, France, 1987) pp. 3-40.
6. M. Aguilar-Benitez *et al.*, Phys. Lett. **135B**, 237 (1984), **189B**, 476 (1987), and Z. Phys. C. to be published.
7. R. Ammar *et al.*, Phys. Lett. **183B**, 110 (1987).
8. A. T. Goshaw, "Charm Production from 400 and 800 GeV/c Proton-Proton Collisions", St. Croix, *loc. cit.*
9. D. W. Duke and J. F. Owens, Phys. Rev. **D30**, 49 (1984).
10. A. D. Martin, R. G. Roberts, and W. J. Stirling, Phys. Rev. **D37**, 1161 (1988).

11. UA1 Collaboration, C. Albajar *et al.* "Measurement of the Bottom Quark Production Cross Section in Proton-Antiproton Collisions at $\sqrt{s} = 0.63$ TeV, CERN-EP/88-100, submitted to Phys. Lett.
12. J. Conboy, "The WA78 Spectrometer", poster session, XXIV International Conference on High Energy Physics, Munich, 1988.
13. M. G. Catanesi *et al.*, Phys. Lett. **187B**, 431 (1987).
14. E. L. Berger, Phys. Rev. **D37**, 1810 (1988).
15. P. Bordalo *et al.*, Z. Phys. **C39**, 7 (1988).
16. UA1 Collaboration, C. Albajar *et al.*, Z. Phys. **C37**, 505 (1988).
17. H. Baer, V. Barger, H. Goldberg, and R. J. N. Phillips, Phys. Rev. **D37**, 3152 (1988); R. Kleiss, A. D. Martin, and W. J. Stirling, Z. Phys. **C39**, 393 (1988); S. Gupta and D. P. Roy, Z. Phys. **C39**, 417 (1988).
18. V. Barger and R. J. N. Phillips, Phys. Lett. **B201**, 553 (1988).
19. I. Bigi and S. Rudaz, Phys. Lett. **153B**, 335 (1985); H. Baer and X. Tata, Phys. Lett. **167B**, 241 (1986).

DISCLAIMER

This report was prepared as an account of work sponsored by an agency of the United States Government. Neither the United States Government nor any agency thereof, nor any of their employees, makes any warranty, express or implied, or assumes any legal liability or responsibility for the accuracy, completeness, or usefulness of any information, apparatus, product, or process disclosed, or represents that its use would not infringe privately owned rights. Reference herein to any specific commercial product, process, or service by trade name, trademark, manufacturer, or otherwise does not necessarily constitute or imply its endorsement, recommendation, or favoring by the United States Government or any agency thereof. The views and opinions of authors expressed herein do not necessarily state or reflect those of the United States Government or any agency thereof.